Dalton Transactions

PAPER

View Article Online
View Journal | View Issue

Cite this: *Dalton Trans.*, 2015, **44**, 12613

12-Metal 36-membered ring based W^V–Co^{II} layers showing spin-glass behavior†

Liang Zhao, Ran Duan, Peng-Fei Zhuang, Hui Zheng, Cheng-Qi Jiao, Jun-Li Wang, Cheng He and Tao Liu*

Received 7th April 2015,
Accepted 27th May 2015

DOI: 10.1039/c5dt01318f

www.rsc.org/dalton

The present study describes the designed synthesis, X-ray structures, and magnetic properties of two 2D cyano bridged heterobimetallic W^V–Co^{II} networks, $\{[W(CN)_8]_2[Co(phpy)_4]_3\}\cdot 2CH_3OH\cdot 2H_2O$ (**1**) and $\{[W(CN)_8]_2[Co(4\text{-spy})_4]_3\}\cdot 6H_2O$ (**2**) (phpy = 4-phenylpyridine, 4-spy = 4-styrylpyridine). Both compounds consist of cyano-bridged 12-metal 36-membered ring units, $Co_6W_6(CN)_{12}$, joined by organic linkers into a 2D plane. The layer presents a corrugated configuration in compound **1** and a plane configuration in compound **2** due to different π–π stacking interactions. Magnetic measurements reveal that both **1** and **2** have a transition to the spin glass-like phase due to competitive magnetic interactions.

Introduction

Cyano-bridged molecular magnetic materials have attracted considerable interest because of their fascinating structure topologies and magnetic properties in the past two decades.[1] Octacyanometallate $[M^V(CN)_8]^{3-}$ (M = Mo and W) was considered as a good candidate for the design of molecule-based magnets because of its non-zero spin state, variable valence, and multiple spatial configurations, such as bicapped trigonal prism (C_{2v}), dodecahedron (D_{2d}) and square antiprism (D_{4d}).[2] The combination of the paramagnetic $[M(CN)_8]^{3-}$ (M = Mo and W) anionic species and transition-metal cations has produced multifarious molecular structures spanning from zero-dimensional discrete molecules (0D), 1D chains, 2D layers, to 3D frameworks,[3] which exhibited photo-induced magnetism,[4] high Curie temperatures,[5] single-chain magnetism and single-molecule magnetism.[6] Among these magnetic materials, W–Co systems were of particular interest because they demonstrate the temperature and light-tunable magnetic bistable state equilibrium, $Co^{II}W^V$ (HS, high-spin) ↔ $Co^{III}W^{IV}$ (LS, low-spin), which was called charge-transfer-induced spin transition (CTIST).[7] Such magnetic materials with tunable bistable states could be a potential basis to construct the molecule nanoswitches. For example, both $Cs^I[\{Co^{II}(3\text{-cyanopyridine})_2\}\{W^V(CN)_8\}]\cdot H_2O$ [8] and $Co^{II}_3[W^V(CN)_8]_2(pyrimidine)_4\cdot 6H_2O$ [9] exhibited a temperature-induced phase transition with a large thermal hysteresis and photo-induced magnetization. Such phenomena were due to the transformation between Co^{II}(S = 3/2)–W^V(S = 1/2) and Co^{III}(S = 0)–W^{IV}(S = 0) phases. Moreover, the high spin cobalt(II) ions possess spin–orbit coupling and strong anisotropy, which have potential to develop magnetic ordering phases,[10] low dimensional single chain magnets[11] or single molecule magnets,[12] ferroelectric networks, spin-crossover compounds,[13] and chiral magnets.[14] Recently, a multifunctional Co^{II}–W^V chain was reported to exhibit both single-chain magnet behavior and chiral properties.[15]

The cyano-bridged molecular magnetic materials have attracted great attention due to their fascinating structure and unique properties. However, it is still a challenge to design and synthesize magnetic coordination polymers containing multi-membered metal rings using metallocyanate as a building block. With $[W^V(CN)_8]^{3-}$, Co^{2+} and organic ligands, we synthesized two 2D compounds $\{[W(CN)_8]_2[Co(phpy)_4]_3\}\cdot 2CH_3OH\cdot 2H_2O$ (**1**) and $\{[W(CN)_8]_2[Co(spy)_4]_3\}\cdot 6H_2O$ (**2**) (phpy = 4-phenylpyridine, 4-spy = 4-styrylpyridine). Both compounds contain cyano-bridged 12 metal 36 membered rings and present spin glass behavior.

Results and discussion

Crystal structure of compounds 1–2

Complex **1** was synthesized by a diffusion method in a test tube. Single-crystal X-ray diffraction analysis revealed that compound **1** crystallized in a monoclinic space group $P2_{(1)}/c$. The unit cell consists of two $[W(CN)_8]^{3-}$ units and three $[Co(phpy)_4]^{2+}$ units, forming CN^- bridged wavy layers along the *ab* plane (Fig. S1 and S3†). The layers consist of 36-membered rings with alternate W^V and Co^{II} ions connected *via*

State Key Laboratory of Fine Chemicals, Dalian University of Technology, Dalian, 116024, China. E-mail: liutao@dlut.edu.cn

†Electronic supplementary information (ESI) available: Fig. S1–S16, Tables S1 and S2. X-ray crystallographic file in CIF format for **1–2**. CCDC 970286 (**1**) and 1057414 (**2**). For ESI and crystallographic data in CIF or other electronic format see DOI: 10.1039/c5dt01318f

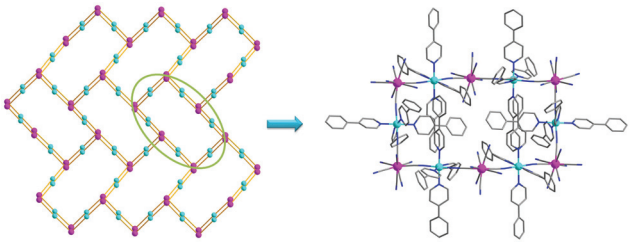

Fig. 1 View of a 2D brick wall like structure with the (6,3) topology of **1** along the *bc* plane (left) and the detailed structure linkage (right). H atoms, water molecules and methanol molecules have been omitted for clarity (W, pink; Co, cyan; C, gray; N, blue).

cyano bridges, exhibiting a normative brick wall topology (Fig. 1). In the layers, the $[W(CN)_8]^{3-}$ unit links three Co^{II} ions through three of its eight cyanide ligands, and each Co^{II} ion is coordinated to two nitrogen atoms from the CN^- in the apical positions and four nitrogen atoms from the 4-phenyl pyridine ligand in the equatorial positions (Fig. S1†). The coordination geometries of the Co^{II} and W^V sites are pseudo-octahedron (D_{4h}) and bicapped trigonal prism (C_2), respectively.[16] At 298 K, the length of the Co–$N_{cyanide}$ bond was 2.12–2.14 Å, and the Co–N_{phpy} bond distances were 2.13–2.21 Å, which were in good agreement with those observed in related compounds containing high spin (HS) Co^{II} ions. The Co–N≡C angles were 173.9–175.95°, departing slightly from linear. The W–C bond distances were 2.16–2.17 Å and the angles of W–C≡N linkages were close to 180°. In the 12-metal ring, three independent Co–W–Co angles are 101.9°, 94.1°, 139.4° and three independent Co–W distances are 5.42, 5.42 and 5.41 Å, respectively. Methanol molecules and H_2O molecules were located between the layers. Hydrogen bonds were formed between the solvent molecules and the 2D layer, with the distances between donor and acceptor being 2.89 Å for N–O and 3.3 Å for O–C (Fig. S7†). The nearest metal–metal distance between the two layers is 14.42 Å.

The structure of compound **2** is similar to that of **1** with the formation of a 2D layer framework (Fig. 2 and S4†). Single-crystal X-ray diffraction analysis shows that compound **2** crystallized a triclinic crystal system $P\bar{1}$ space group. The asymmetric unit is composed of two $[W(CN)_8]^{3-}$ units and three $[Co(spy)_4]^{2+}$ units. The coordination geometries of the Co^{II} ions were pseudo-octahedron (D_{4h}) with two cyanide nitrogen atoms of $[W(CN)_8]^{3-}$ occupying its axial positions and four nitrogen atoms of 4-styrylpyridine occupying the equatorial positions (Fig. S2†). The Co–$N_{cyanide}$ distances are 2.09–2.13 Å, while Co–N_{spy} distances range from 2.15 to 2.21 Å. The Co–N–C angles are 171.8–172.4°. The coordination geometry of the W site was a distorted square antiprism (D_{4d}). Three CN^- groups of $[W^V(CN)_8]^{3-}$ were bridged to three Co atoms, and five other CN^- groups were free. The W–C bond distance ranges from 2.13 to 2.17 Å, and the W–C–N angles have a slightly diverged linearity, with a maximum 5.9° deviation to 180°. The three Co–W–Co angles are 132.8°, 89.4° and 136.5°. The uncoordinated water molecules were located between the layers, forming hydrogen bonds and linking the layers (Fig. S8†). The distances between nitrogen atoms of terminal cyanides and oxygen atoms of water molecules were 2.91–3.01 Å, and the distances between oxygen atoms of water molecules were 3.38–3.4 Å.

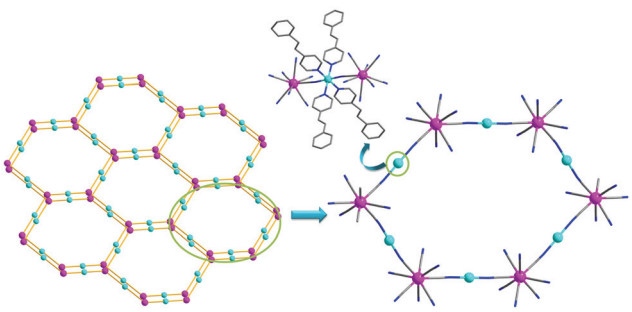

Fig. 2 Crystal structure of **2**, the hydrogen atoms and water molecules have been omitted for clarity (W, pink; Co, cyan; C, gray; N, blue).

The different structures of **1** and **2** come from the weak π–π interaction which can display an important role in controlling the packing or assembly of compounds.[17] The usual π interaction is an offset or slipped stacking of the benzene rings or aromatic nitrogen heterocycles, and the effective distance is about 3.3–3.8 Å. In compound **1**, the π–π interaction exists between the adjacent 4-phenylpyridine ligands belonging to same or different 12-metal rings. The distances (3.14 and 3.49 Å) were in the normal range of the range for such interactions (Fig. S5†). The weak interaction indirectly influences the coordination mode of W–C≡N–Co. The sum of the three independent Co–W–Co angles is 335.4°, much less than 360°. The four atoms are not in a plane and have some radian, which leads the plane to be tortuous. However, the π–π staking interaction only appeared in the same 12-metal rings in compound **2** (Fig. S6†), and the sum of the three independent Co–W–Co angles is 358.7°, so the plane was smooth.

Magnetic studies

Variable-temperature magnetic measurements were performed on monocrystalline samples of compound **1** in the range of 1.8–300 K in 1000 Oe, as shown in Fig. 3a. The χT value per W^VCo^{II} unit was 9.78 $cm^3\ mol^{-1}$ K at 300 K. This value was higher than the spin-only value expected for two isolated W^V of $S = 1/2$ ($g = 2$) and three Co^{II} of $S = 3/2$ ($g = 2.0$) due to the orbital contributions of Co^{II} ions.[18] The magnetic susceptibility data follow a Curie–Weiss law in the temperature range 15–300 K with a positive Weiss temperature θ = 19.4 K and Curie constant C = 9.25 $cm^3\ mol^{-1}$ K. The positive Weiss temperature suggests that dominant ferromagnetic interactions were transmitted through the cyanide bridge, which results from the orthogonality of the magnetic orbital through the π orbital of the e_g–t_{2g} pathway, as the electronic configurations are t_{2g}^1 and $t_{2g}^5e_g^2$ for W^V and Co^{II}, respectively. Upon cooling, the χT value gradually increased to a sharp maximum of 291 $cm^3\ mol^{-1}$ K around 11.0 K, confirming the strong ferro-

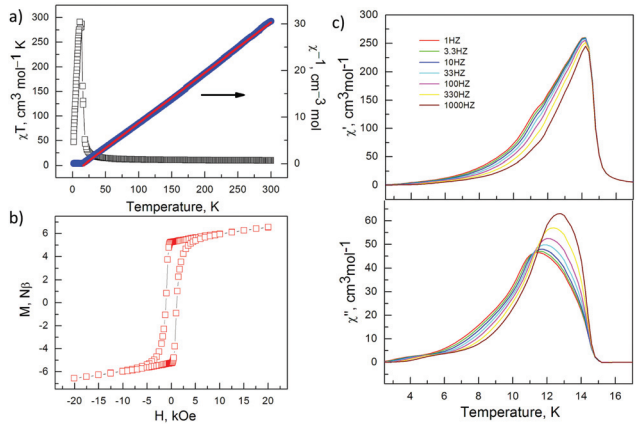

Fig. 3 (a) Temperature-dependent magnetic susceptibilities of compound **1** in the temperature range of 2–300 K under an applied field of 1 kOe. The red solid line is the fitting to the Curie–Weiss law. (b) Field dependence of magnetization of compound **1** at 2 K. (c) Temperature dependence of the real part and the imaginary part of the ac susceptibility of **1** in a zero dc field and a 3.5 Oe ac field.

magnetic interactions between W^V and Co^{II}. As the temperature further lowered, the χT value dropped sharply to 46.9 cm^3 mol^{-1} K at 1.8 K. The sudden decrease in χT was attributed to the presence of zero-field splitting and/or antiferromagnetic interactions.

The field-dependent magnetization of compound **1** was measured up to 50 kOe at 2 K. As shown in Fig. S9,† the magnetization increases rapidly in the low field region and reaches $5.2N\beta$ at H = 300 Oe, and then keeps increasing slowly and reaches $8.1N\beta$ at 50 kOe without saturation (per Co_3W_2 unit). Such data are consistent with other reported cyano-bridged $Co^{II}_3W^V_2$ networks.[13c,14a,19] In order to further explore the switching or reversal of the magnetization with applied field, the full hysteresis loops were recorded at 2 K. As shown in Fig. 3b, compound **1** exhibited an obvious hysteresis with a remnant magnetization (M_r) of $5.45N\beta$ and a coercive field (H_c) of 1040 Oe. The zero-field-cooled (ZFC) and field-cooled (FC) magnetization measurements were performed for **1** at 10 Oe in the 2–25 K range to research the phase transformation at low temperatures. The ZFC and FC curves show a divergence at 14.0 K, indicating the existence of spontaneous magnetization blow 14.0 K (Fig. S10†).

The ac susceptibility was measured in the frequency range of 1–1000 Hz at 2–20 K to investigate the dynamic nature of compound **1** (Fig. 3c). Both in-phase χ' and out-of phase χ'' susceptibility signals were frequency dependent below 14.4 K. The parameter $\phi = (\Delta T_p/T_p)/\Delta(\log f)$, a measure of the frequency dependence of the peak temperature shift (ΔT_p) of χ'', was estimated to be 0.065, located in the region of canonical spin-glass behavior ($\phi \leq 0.1$).[21] Moreover, the relaxation rate can be simulated by the Arrhenius equation $\tau = \tau_0 \exp(\Delta/k_BT)$, where $\tau = 1/2\pi\nu$ and τ_0 was a pre-exponential factor. Least-squares fitting gives $\tau_0 = 1.50 \times 10^{-25}$ s and Δ/k_B = 620 K (Fig. S13†). The rather small value of τ_0 obviously indicates the characteristic of spin-glass phase as well.[20] On the other hand, another quantitative measurement was acquired by fitting the frequency dependence maxima in χ''. The conventional critical scaling law of the spin dynamics, $\tau = \tau_0[(T_p - T_f)/T_f]^{-z\nu}$, was used in the spin glass system. τ is the relaxation time, T_f is the freezing temperature, T_p is the spin glass temperature, and $z\nu$ is the critical exponent. The fitting results give the parameters $\tau_0 = 7.17 \times 10^{-9}$ s, T_f = 10.96 K, and $z\nu$ = 5.19 (Fig. S15†). The value of $z\nu$ is in the range of various spin glass behaviors from 4 to 12.[21] All ac magnetic measurements and derived results confirm the canonical spin glasses for compound **1**.

The temperature dependence of the χT values of **2** under 1 kOe is displayed in Fig. 4a. The χT value per W^VCo^{II} unit was 9.85 cm^3 mol^{-1} K at 300 K, being significantly higher than the spin-only value of 6.38 cm^3 mol^{-1} K expected for two isolated W^V of S = 1/2 (g = 2) and three Co(II) of S = 3/2 (g = 2.0) due to the orbital contributions of Co^{II} ions. As the temperature lowered, the transforming tendency in the χT *vs.* T curve was similar to that of **1**. The plots of $1/\chi$ *vs.* T above 30 K were fitted to the Curie–Weiss law, giving θ = 12.05 K and C = 9.39 cm^3 mol^{-1} K. It suggests dominant ferromagnetic interactions between W^V and Co^{II}. The sudden decrease in χT in the low temperature region was attributed to the presence of zero-field splitting and/or antiferromagnetic interactions. As shown in Fig. S11,† magnetization of compound **2** reaches $8.38N\beta$ at 50 kOe without saturation. The M_r and H_c were $5.7N\beta$ and 330 Oe, respectively, at 2 K (Fig. 4b). The ZFC and FC magnetization data at a low field of 20 Oe displayed irreversibility below 6.5 K (Fig. S12†), indicating a blocking of the magnetization due to the presence of a barrier.

AC susceptibility measurements of compound **2** show that both χ' and χ'' susceptibility signals display obvious frequency dependence below 6.5 K (Fig. 4c). The parameter $\phi = (\Delta T_p/T_p)/\Delta(\log f) = 0.087$ was consistent with canonical spin-glass be-

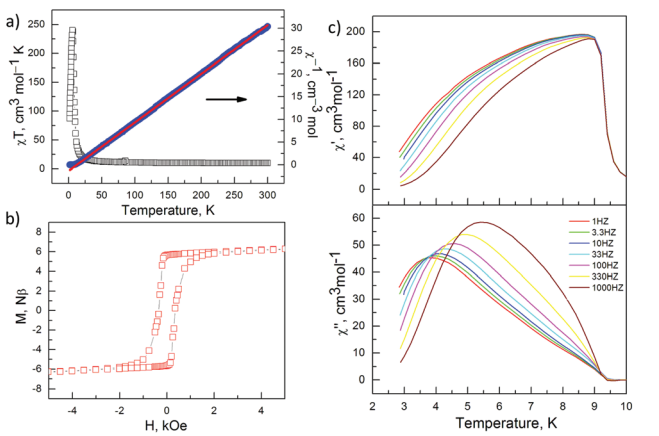

Fig. 4 (a) Temperature-dependent magnetic susceptibilities of compound **2** in the temperature range of 2–300 K under an applied field of 1 kOe. The red solid line is the fitting to the Curie–Weiss law. (b) Field dependence of magnetization of compound **2** at 2 K. (c) Temperature dependence of the real part and the imaginary part of the ac susceptibility of **2** in a zero dc field and a 3.5 Oe ac field.

havior. The best-fit parameters of the Arrhenius equation were $\tau_0 = 1.16 \times 10^{-12}$ s and $\Delta/k_B = 97.01$ K (Fig. S14†). Another quantitative measurement is obtained by fitting the data with the conventional critical scaling law, $\tau = \tau_0[(T_p - T_f)/T_f]^{-z\nu}$, yielding $\tau_0 = 2.0 \times 10^{-5}$ s, $T_f = 3.17$ K, and $z\nu = 5.89$ (Fig. S16†). The value of $z\nu$ is characteristic of spin glass behavior. The randomness (disorder, defects, *etc.*) and frustration (competitive or geometrical) are responsible for the spin-glass system, which always have been caused by the antiferromagnetic interaction between different structural units.[22] In compounds **1** and **2**, the hydrogen bonding interaction between the different layers can cause a weak antiferromagnetic coupling interaction. The spin-glass behavior may come from competing intralayer ferromagnetic interactions and interlayer antiferromagnetic interactions.

Conclusions

In conclusion, two cyano-bridged bimetallic W^V–Co^{II} layers have been prepared and characterized, in which the 12-metal 36-membered ring, $Co_6W_6(CN)_{12}$, is the fundamental building unit. Compound **1** shows a wavy-like structural plane, whereas a smoother plane exists in compound **2** due to different types of π–π stacking interactions. Magnetic studies reveal that both compounds exhibit spin glass behavior.

Experimental

Materials and methods

All chemical reagents were acquired from commercial sources and were used as received without further purification. $(Bu_4N)_3W(CN)_8{\cdot}2H_2O$ was synthesized according to the modified literature method.[23] Elemental analyses were performed on an Elementar Vario EL III analyzer. Magnetic measurements of the samples were performed on a Quantum Design SQUID (MPMS XL-7) magnetometer. Data were corrected for the diamagnetic contribution calculated from Pascal constants.

Synthesis of $\{[W(CN)_8]_2[Co(4\text{-phenylpyridine})_4]_3\}{\cdot}2CH_3OH{\cdot}2H_2O$ (1). A 6.0 mL aqueous solution of $Co(ClO_4)_2{\cdot}6H_2O$ (0.03 mmol) was placed at the bottom of a test tube; a mixture of methanol and water (1 : 2, v/v, 6 mL) was gently layered on the top of the solution, and then a 6.0 mL methanol solution of $(Bu_4N)_3W(CN)_8{\cdot}2H_2O$ (0.02 mmol) and 4-phenylpyridine (0.12 mmol) was carefully added as the third layer. After a few weeks, dark red block crystals of **1** suitable for X-ray measurements were collected, washed with water and air dried. Yield: 62% based on $Co(ClO_4)_2{\cdot}6H_2O$. Anal. calcd (%) for $C_{150}H_{120}Co_3N_{28}O_4W_2$: C 61.63, H 4.14, N 13.42; found: C 61.50, H 4.27, N 13.34.

Synthesis of $\{[W(CN)_8]_2[Co(4\text{-styrylpyridine})_4]_3\}{\cdot}6H_2O$ (2). The compound was obtained with a similar procedure to that of **1**. 4-Styrylpyridine was used instead of 4-phenylpyridine. The red precipitated powder was formed immediately and the filtrate was also left in the dark for crystallization. The black red crystal for measurements was collected after several weeks. Yield: 55% based on $Co(ClO_4)_2{\cdot}6H_2O$. Anal. calcd (%) for $C_{172}H_{144}Co_3N_{28}O_6W_2$: C 63.69, H 4.47, N 12.09; found: C 63.80, H 4.52, N 12.21.

Crystallography

The data were collected on a Bruker Smart APEX II X-diffractometer equipped with graphite monochromated Mo-Kα radiation ($\lambda = 0.71073$ Å) using the SMART and SAINT programs at 298 K for **1** and 180 K for **2**. Final unit cell parameters were based on all observed reflections from the integration of all frame data. The structures were solved in the space group by direct methods and refined by the full-matrix least-squares using SHELXTL-97 fitting on F^2.[24] Anisotropic thermal parameters were used for all the non-hydrogen atoms except for the disordered water molecule of **1**. Hydrogen atoms bound to carbon were added geometrically and refined using a mixed model for **1** and constant model for **2**. Attempts to add the hydrogen atoms for the solvent water molecules in the crystal structure of compounds through Fourier electron density failed. However, no attempts were made to fix these atoms on their parents.

Acknowledgements

This work was supported by the National Natural Science Foundation of China (Grants 21421005, 21322103, 91422302, and 91122031).

Notes and references

1 (*a*) O. Sato, J. Tao and Y.-Z. Zhang, *Angew. Chem., Int. Ed.*, 2007, **46**, 2152; (*b*) N. Ozaki, H. Tokoro, Y. Hamada, A. Namai, T. Matsuda, S. Kaneko and S.-i. Ohkoshi, *Adv. Funct. Mater.*, 2012, **22**, 2089; (*c*) T. Liu, Y. J. Zhang, S. Kanegawa and O. Sato, *Angew. Chem., Int. Ed.*, 2010, **49**, 8645.

2 (*a*) T. W. Wang, J. Wang, S. Ohkoshi, Y. Song and X. Z. You, *Inorg. Chem.*, 2010, **49**, 7756; (*b*) A. H. Yuan, S. Y. Qian, W. Y. Liu, H. Zhou and Y. Song, *Dalton Trans.*, 2011, **40**, 5302.

3 (*a*) W. Kosaka, K. Imoto, Y. Tsunobuchi and S.-i. Ohkoshi, *Inorg. Chem.*, 2009, **48**, 4604; (*b*) K. Tomono, Y. Tsunobuchi, K. Nakabayashi and S.-i. Ohkoshi, *Inorg. Chem.*, 2010, **49**, 1298; (*c*) J. Qian, H. Yoshikawa, J. Zhang, H. Zhao, K. Awaga and C. Zhang, *Cryst. Growth Des.*, 2009, **9**, 5351; (*d*) Q. Zhang, G. Zhu, X. Shen, L. Tong, Z. Ye and K. Chen, *CrystEngComm*, 2013, **15**, 2909.

4 (*a*) T. Liu, H. Zheng, S. Kang, Y. Shiota, S. Hayami, M. Mito, O. Sato, K. Yoshizawa, S. Kanegawa and C. Duan, *Nat. Commun.*, 2013, **4**, 2826; (*b*) D. P. Dong, T. Liu, S. Kanegawa, S. Kang, O. Sato, C. He and C. Y. Duan, *Angew. Chem., Int. Ed.*, 2012, **51**, 5119; (*c*) M. Shatruk,

A. Dragulescu-Andrasi, K. E. Chambers, S. A. Stoian, E. L. Bominaar, C. Achim and K. R. Dunbar, *J. Am. Chem. Soc.*, 2007, **129**, 6104; (*d*) J. M. Herrera, V. Marvaud, M. Verdaguer, J. Marrot, M. Kalisz and C. Mathoniere, *Angew. Chem., Int. Ed.*, 2004, **43**, 5468.

5 (*a*) S.-i. Ohkoshi, Y. Tsunobuchi, H. Takahashi, T. Hozumi, M. Shiro and K. Hashimoto, *J. Am. Chem. Soc.*, 2007, **129**, 3084; (*b*) J. R. Withers, D. Li, J. Triplet, C. Ruschman, S. Parkin, G. Wang, G. T. Yee and S. M. Holmes, *Inorg. Chem.*, 2006, **45**, 4307; (*c*) D. Pinkowicz, R. Podgajny, M. Bałanda, M. Makarewicz, B. Gaweł, W. Łasocha and B. Sieklucka, *Inorg. Chem.*, 2008, **47**, 9745.

6 (*a*) J. Wang, Y. L. Xu, H. B. Zhou, H. S. Wang, X. J. Song, Y. Song and X. Z. You, *Dalton Trans.*, 2010, **39**, 3489; (*b*) N. Bridonneau, L. M. Chamoreau, P. P. Laine, W. Wernsdorfer and V. Marvaud, *Chem. Commun.*, 2013, **49**, 9476.

7 A. Mondal, L. M. Chamoreau, Y. Li, Y. Journaux, M. Seuleiman and R. Lescouezec, *Chem. – Eur. J.*, 2013, **19**, 7682.

8 Y. Arimoto, S.-i. Ohkoshi, Z. J. Zhong, H. Seino, Y. Mizobe and K. Hashimoto, *J. Am. Chem. Soc.*, 2003, **125**, 9240.

9 S.-i. Ohkoshi, S. Ikeda, T. Hozumi, T. Kashiwagi and K. Hashimoto, *J. Am. Chem. Soc.*, 2006, **128**, 5320.

10 (*a*) R. Podgajny, M. Balanda, M. Sikora, M. Borowiec, L. Spalek, C. Kapusta and B. Sieklucka, *Dalton Trans.*, 2006, 2801, DOI: 10.1039/b516004a; (*b*) Y.-Z. Tong, Q.-L. Wang, C.-Y. Su, Y. Ma, S. Ren, G.-F. Xu, G.-M. Yang, P. Cheng and D.-Z. Liao, *CrystEngComm*, 2013, **15**, 9906.

11 S.-L. Ma, S. Ren, Y. Ma, D.-Z. Liao and S.-P. Yan, *Struct. Chem.*, 2009, **20**, 161.

12 J. H. Yoon, J. W. Lee, D. W. Ryu, S. Y. Choi, S. W. Yoon, B. J. Suh, E. K. Koh, H. C. Kim and C. S. Hong, *Inorg. Chem.*, 2011, **50**, 11306.

13 (*a*) S. Ohkoshi, K. Imoto, Y. Tsunobuchi, S. Takano and H. Tokoro, *Nat. Chem.*, 2011, **3**, 564; (*b*) F. Habib, O. R. Luca, V. Vieru, M. Shiddiq, I. Korobkov, S. I. Gorelsky, M. K. Takase, L. F. Chibotaru, S. Hill, R. H. Crabtree and M. Murugesu, *Angew. Chem., Int. Ed.*, 2013, **52**, 11290; (*c*) D. Pinkowicz, M. Rams, W. Nitek, B. Czarnecki and B. Sieklucka, *Chem. Commun.*, 2012, **48**, 8323.

14 (*a*) J. M. Herrera, A. Bleuzen, Y. Dromzée, M. Julve, F. Lloret and M. Verdaguer, *Inorg. Chem.*, 2003, **42**, 7052; (*b*) R. Podgajny, S. Chorazy, W. Nitek, M. Rams, A. M. Majcher, B. Marszalek, J. Zukrowski, C. Kapusta and B. Sieklucka, *Angew. Chem., Int. Ed.*, 2013, **52**, 896; (*c*) S. Chorazy, R. Podgajny, A. M. Majcher, W. Nitek, M. Rams, E. A. Suturina, L. Ungur, L. F. Chibotaru and B. Sieklucka, *CrystEngComm*, 2013, **15**, 2378.

15 (*a*) S. Chorazy, K. Nakabayashi, K. Imoto, J. Mlynarski, B. Sieklucka and S. Ohkoshi, *J. Am. Chem. Soc.*, 2012, **134**, 16151; (*b*) K. Komori Orisaku, K. Nakabayashi and S.-i. Ohkoshi, *Chem. Lett.*, 2011, **40**, 586.

16 D. Visinescu, C. Desplanches, I. Imaz, V. Bahers, R. Pradhan, F. A. Villamena, P. Guionneau and J.-P. Sutter, *J. Am. Chem. Soc.*, 2006, **128**, 10202.

17 C. Janiak, *J. Chem. Soc., Dalton Trans.*, 2000, 3885, DOI: 10.1039/b003010o.

18 F. Lloret, M. Julve, J. Cano, R. Ruiz-García and E. Pardo, *Inorg. Chim. Acta*, 2008, **361**, 3432.

19 S.-i. Ohkoshi, Y. Hamada, T. Matsuda, Y. Tsunobuchi and H. Tokoro, *Chem. Mater.*, 2008, **20**, 3048.

20 J. A. Mydosh, *Spin Glasses: An Experimental Introduction*, Taylor & Francis, London, 1993.

21 (*a*) M. X. Yao, Q. Zheng, X. M. Cai, Y. Z. Li, Y. Song and J. L. Zuo, *Inorg. Chem.*, 2012, **51**, 2140; (*b*) Y. Q. Wang, Q. Yue, Y. Qi, K. Wang, Q. Sun and E. Q. Gao, *Inorg. Chem.*, 2013, **52**, 4259; (*c*) J. Li, B. Li, P. Huang, H. Y. Shi, R. B. Huang, L. S. Zheng and J. Tao, *Inorg. Chem.*, 2013, **52**, 11573.

22 (*a*) X. Liu, P. Cen, H. Li, H. Ke, S. Zhang, Q. Wei, G. Xie, S. Chen and S. Gao, *Inorg. Chem.*, 2014, **53**, 8088; (*b*) F. J. Klinke, A. Das, S. Demeshko, S. Dechert and F. Meyer, *Inorg. Chem.*, 2014, **53**, 2976; (*c*) K. Nakabayashi, S. Chorazy, D. Takahashi, T. Kinoshita, B. Sieklucka and S.-i. Ohkoshi, *Cryst. Growth Des.*, 2014, **14**, 6093; (*d*) A. K. Ghosh, M. Shatruk, V. Bertolasi, K. Pramanik and D. Ray, *Inorg. Chem.*, 2013, **52**, 13894.

23 L. D. C. Bok, J. G. Leipoldt and S. S. Basson, *Z. Anorg. Allg. Chem.*, 1975, **415**, 81.

24 G. M. Sheldrick, *SHELXL-97, Program for X-ray Crystal Structure Refinement*, University of Göttingen, Göttingen, 1997.